

# Control of free space propagation of Airy beams generated by quadratic nonlinear photonic crystals

Ido Dolev,<sup>a)</sup> Tal Ellenbogen,<sup>b)</sup> Noa Voloch-Bloch,<sup>c)</sup> and Ady Arie<sup>d)</sup>

Department of Physical Electronics, Fleischman Faculty of Engineering, Tel-Aviv University, Tel-Aviv 69978, Israel

(Received 18 October 2009; accepted 21 October 2009; published online 20 November 2009)

We present experimentally the control of free space propagation of an Airy beam. This beam is generated by a nonlinear wave mixing process in an asymmetrically poled nonlinear photonic crystal. Changing the quasi-phase matching conditions, e.g., the crystal temperature or pump wavelength, alters the location of the Airy beam peak intensity along the same curved trajectory. We explain that the variation in the beam shape is caused by noncollinear interactions. Owing to the highly asymmetric shape of nonlinear crystal in the Fourier space, these noncollinear interactions are still relatively efficient for positive (nonzero) phase mismatch. © 2009 American Institute of Physics. [doi:10.1063/1.3266066]

It was shown in 1979 by Berry and Balazs<sup>1</sup> that the free particle Schrödinger equation has a nonspreading Airy wave packet solution. The mathematical analog of Schrödinger equation in quantum mechanics and the paraxial equation for electromagnetic waves allows the experimental realization of Airy beams in the field of optics.<sup>2,3</sup> Airy beams have several unique properties. The envelope of these beams is centered around a parabolic trajectory in space and they are considered nearly diffraction-free and self healing, i.e., self restoring their canonical form after passing small obstacles.<sup>4</sup> The evolution of the Poynting vector<sup>5</sup> and the ballistic dynamics of these beams were analyzed<sup>6</sup> and it was shown that the unique properties of Airy beams may be useful for optical micromanipulation of small particles<sup>7</sup> and for generation of curved plasma channels in air.<sup>8</sup>

Recently a method for generating Airy beams by a second harmonic generation (SHG) process in unique two dimensional nonlinear photonic crystal was demonstrated.<sup>9</sup> In that work, it was suggested theoretically that the generation of Airy beams by nonlinear processes opens several possibilities for controlling and manipulating these beams.<sup>9</sup> Here we experimentally demonstrate a method to control the relative intensity along the caustic of nonlinearly generated Airy beams, by controlling the phase matching (PM) conditions of the nonlinear interaction via temperature tuning. By analyzing the interactions in the Fourier space, we show that the shaping of the beams is achieved by having noncollinear interactions. Furthermore, we study the possibilities for all-optical control by changing the pump wavelength.

The design and fabrication of the asymmetric quadratic nonlinear photonic structure were described in Ref. 9. The binary designed space-dependent quadratic nonlinear coefficient is based on periodic modulation in the propagation direction and cubic modulation in the transverse direction, in the form  $d_{ij} \text{sign}\{\cos(2\pi f_x x + f_c y^3)\}$ , where  $d_{ij}$  is an element of the quadratic susceptibility tensor. Efficient collinear second harmonic generation occurs in this crystal if the wave-

vector mismatch  $k_2 - 2k_1$  is compensated by the longitudinal crystal's reciprocal lattice vector  $g_x = 2\pi f_x$ , where  $k_1$  and  $k_2$  are the wave vectors of the first and SH waves. The Y component of the nonlinear coefficient modulation imposes a cubic phase in the transverse direction.<sup>9</sup> Performing an optical Fourier transform (FT) to the SH wave, by using a lens, results in an accelerating Airy beam.<sup>2</sup>

One of the main advantages of this nonlinear photonic crystal is the ability to shape the caustic of the generated Airy beam, by changing the crystal temperature or pump wavelength. In order to understand this effect, it is useful to analyze the nonlinear process in the Fourier space. The calculated Fourier space [Fig. 1(a)] consists of two Airy functions in the  $+f_y$  and  $-f_y$  directions, at a spatial frequencies  $\pm 2\pi f_x$ . This structure supports QPM of both collinear and noncollinear interactions (as illustrated by the arrows). Figures 1(c) and 1(d) illustrate the k vectors in the cases of collinear and noncollinear SHG, respectively. Here we assume that the process is collinearly phase-matched for a certain pump wavelength and crystal temperature. Altering any one of these parameters may result in a process which is noncollinearly phase-matched. Given that the crystal length  $L$  is finite, the nonlinear process may be efficient even for a relatively small mismatch of up to  $\pm 2\pi/L$ . For example, in the plane-wave approximation the efficiency is proportional to  $\text{sinc}^2(\Delta k L/2)$  where  $\Delta k = \min(|2\vec{k}_\omega + \vec{g} - \vec{k}_{2\omega}|)$  for all the reciprocal lattice vectors,  $\vec{g}$ , induced by the crystal. Since the FT of the crystal consists of a truncated Airy function in the X axis, the efficiencies of the  $k_{2\omega}$  vectors that can be simultaneously phase-matched are the product of this truncated Airy function with the  $\text{sinc}^2(\Delta k L/2)$  efficiency.

In the collinear case [Fig. 1(c)] the total efficiency window is centered at  $k_y = 0$ , it is reaching to  $k_y = \sqrt{|\vec{k}_{2\omega}|^2 - [2|\vec{k}_\omega| + g_x - (2\pi/L)]^2}$ , and the product gives a truncated Airy function [Fig. 1(e)]. On the other hand, in the noncollinear case [Fig. 1(d)], the center of efficiency window is at  $\vec{k}_{2\omega} = 2\vec{k}_\omega + \vec{g}$ , ( $k_y \neq 0$ ), and it is spreading from  $k_y = \sqrt{|\vec{k}_{2\omega}|^2 - [2|\vec{k}_\omega| + g_x + (2\pi/L)]^2}$  to  $k_y = \sqrt{|\vec{k}_{2\omega}|^2 - [2|\vec{k}_\omega| + g_x - (2\pi/L)]^2}$ . As a result a different set of  $k_{2\omega}$  vectors obey the phase matching requirement and the

<sup>a)</sup> Author to whom correspondence should be addressed. Tel.: +972-54-2300094. Electronic mail: idodolev@post.tau.ac.il.

<sup>b)</sup> Tel.: +972-3-6408271. Electronic mail: ellenbog@post.tau.ac.il.

<sup>c)</sup> Tel.: +972-3-6407545. Electronic mail: noavoloch@gmail.com.

<sup>d)</sup> Tel.: +972-3-6406627. Electronic mail: ady@eng.tau.ac.il.

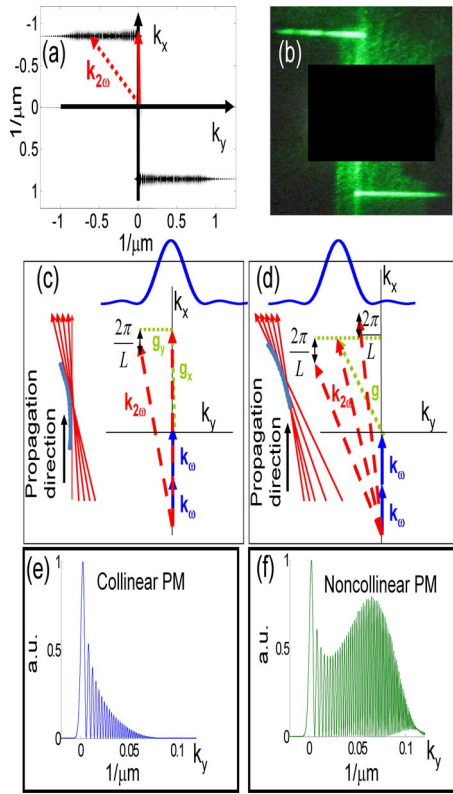


FIG. 1. (Color online) (a) Calculated Fourier space. (b) Measured far field diffraction pattern (central part blocked). [(c) and (d)] Collinear and noncollinear processes, respectively. The efficient interaction area, in  $k$  space, is illustrated by the  $\text{sinc}^2(\Delta kL/2)$ . The arrows illustrate the  $k$  vectors of the pump (solid), SH (dashed) and the crystal (dots). [(e) and (f)] Truncated Airy function multiplied by the efficiency window, collinear and noncollinear PM, respectively.

shape of the truncated Airy function is changed [Fig. 1(f)]. This has a very significant effect on the caustics of the generated beams, as illustrated in the insets of Figs. 1(c) and 1(d).

This behavior is similar to what happens to an Airy beam when part of it is blocked by an obstacle, which eliminates part of the  $k$  vectors of the beam. After a certain propagation distance, the beam will return to its canonical form.<sup>4</sup> Here, we can control this effect by varying the QPM conditions, which can be done either by temperature tuning or all-optically, by changing the pump wavelength.

For crystal preparation we used the electric field poling technique<sup>10</sup> to modulate the nonlinear coefficient of a 1 mm long MgO doped stoichiometric lithium tantalite. The modulation period in the propagation direction  $1/f_x$  was  $7.38 \mu\text{m}$  and the cubic modulation coefficient  $f_c$  was  $1.9 \times 10^{-7} \mu\text{m}^{-3}$ . The selectively etched crystal was tested by observing its diffraction pattern with 532 nm laser beam, as shown in Fig. 1(b), which is in excellent agreement with the calculated FT, Fig. 1(a). The measured first order diffraction angle is obtained at  $4.1^\circ \pm 0.1^\circ$ , which fits exactly to the designed poling period ( $7.38 \mu\text{m}$ ). We generated the SH from a single mode Gaussian Nd:YLF 1047.5 nm pump laser weakly focused in the middle of the modulated crystal with waist radii of  $\sim 700$  and  $45 \mu\text{m}$  in the crystallographic Y and Z directions, respectively. The crystal was placed on a temperature controlled oven with accuracy of  $0.1^\circ\text{C}$ . We used a lens of 100 mm focal length after the crystal to perform an optical FT.

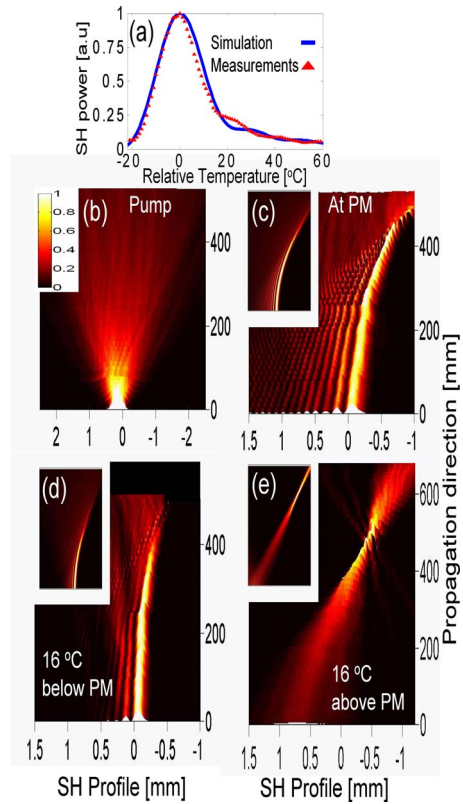


FIG. 2. (Color online) Shaping the caustic of the generated Airy wave packet by changing crystal temperature. Beams propagate from bottom to top, normalized scale. (a) Split-step Fourier simulation and experimental SH efficiency vs. relative temperature (with respect to PM temperature). (b) Output pump wave. [(c), (d), and (e)] SH experimental results, inset: simulation results.

The experimental measurements were compared to a numerical simulation based on the split-step Fourier method.<sup>11</sup> The peak power of the SH was measured at  $120^\circ\text{C}$ . Although the temperature predicted by the Sellmeier equation is  $153^\circ\text{C}$ ,<sup>12</sup> there is a good agreement in the tuning properties between the simulation and the experimental results [Fig. 2(a)]. We then recorded, using PixeLINK charge-coupled device digital camera, the propagation dynamics of the optically FT of the SH output beams at different temperatures and compared the results to simulation. Figure 2(b) presents the experimental results for the propagation of the pump beam after the crystal, Fig. 2(d) is the normalized SH wave at  $16^\circ\text{C}$  below the PM temperature ( $\Delta kL/2 = -0.59\pi$ ), Fig. 2(c) at PM temperature and Fig. 2(e)  $16^\circ\text{C}$  above PM temperature ( $\Delta kL/2 = 0.80\pi$ ). The normalized output pump wave shows the familiar diffraction of a Gaussian beam, while the output SH beam shows different intensity profile for each temperature. At PM the propagation dynamics is of a truncated Airy beam, i.e., nearly nondiffracting and freely accelerating while above PM, the relative peak power of the Airy beam is placed at the “tip end” of the beam. On the other hand, below PM, the propagation dynamics is again in the form of Airy beam but with reduced nondiffracting distance. The highly asymmetric shape of the nonlinearity in the Fourier space leads to distinct differences between the generated beams below PM and above PM. The results fit well to the simulation [Figs. 2(c)–2(e) insets] and the slight deviation is probably due to misalignment between the beam

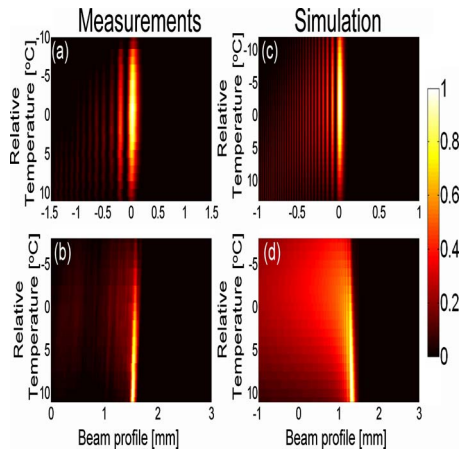


FIG. 3. (Color online) Temperature tuning of the nonlinear interaction. Experimental [(a) and (b)] and simulation [(c) and (d)] results for the SH main lobe normalized intensity pattern vs temperature at focal plane [(a) and (c)] and at 470 mm [(b) and (d)], respectively.

and the camera, and to a small difference in the actual phase mismatch values.

Figure 3 shows the calculated and measured beam profile versus temperature at different locations along beam trajectory, at the focal plane (0 mm) and at 470 mm along the propagation direction. The highest intensity in the focal plane is achieved at PM. However, at a distance of 470 mm from the focal plane, the highest intensity is reached when the crystal temperature is 10 °C above PM. We deduce that although the maximum of the total output power is at PM, at non PM conditions the unique SH profile at the end of the crystal will buildup a maximum output power at different points along beam trajectory.

This control of Airy beams can be also implemented by changing the pump wavelength. Assuming the same crystal parameters, we simulated the effect of pump wavelength tuning in the range of 5 nm around PM (thereby changing  $\Delta kL/2$  from  $-\pi$  to  $+\pi$ ) see Fig. 4. (Media 1, enhanced online). Hence, all-optical control of Airy beams, using a tunable light source, can be realized.

In conclusion, generation of Airy beams by nonlinear quadratic crystals allows unique manipulation capabilities.

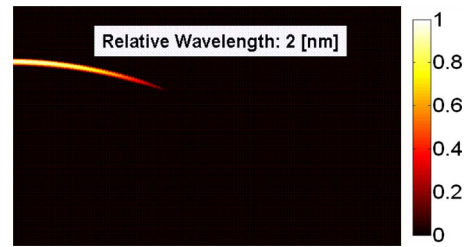


FIG. 4. (Color online) Single-frame excerpts from video. Simulation of all-optical control of Airy beams (wavelength relative to PM: 1047.5 nm). Beam propagates from left to right, normalized scale, all values lower than half maximum were eliminated for viewing purposes (enhanced online). [URL: <http://dx.doi.org/10.1063/1.3266066.1>]

We explained the physical origin of this effect and characterized the propagation dynamics of the generated Airy beams for different phase matching conditions which were imposed by changing the temperature of the crystal. There is a good agreement between the experimental results and the simulations. In addition, we have demonstrated by simulations all-optical Airy beam caustic shaping by a tunable pump light source.

We thank A. Ganany-Padowicz for the preparation of the crystal. This work was supported by the Israel Science Foundation Grant No. 960/05 and by the Israeli Ministry of Science.

- <sup>1</sup>M. V. Berry and N. L. Balazs, *Am. J. Phys.* **47**, 264 (1979).
- <sup>2</sup>G. A. Siviloglou, J. Broky, A. Dogariu, and D. N. Christodoulides, *Phys. Rev. Lett.* **99**, 213901 (2007).
- <sup>3</sup>G. A. Siviloglou and D. N. Christodoulides, *Opt. Lett.* **32**, 979 (2007).
- <sup>4</sup>J. Broky, G. A. Siviloglou, A. Dogariu, and D. N. Christodoulides, *Opt. Express* **16**, 12880 (2008).
- <sup>5</sup>H. I. Sztul and R. R. Alfano, *Opt. Express* **16**, 9411 (2008).
- <sup>6</sup>G. A. Siviloglou, J. Broky, A. Dogariu, and D. N. Christodoulides, *Opt. Lett.* **33**, 207 (2008).
- <sup>7</sup>J. Baumgartl, M. Mazilu, and K. Dholakia, *Nat. Photonics* **2**, 675 (2008).
- <sup>8</sup>P. Polynkin, M. Kolesik, J. V. Moloney, G. A. Siviloglou, and D. N. Christodoulides, *Science* **324**, 229 (2009).
- <sup>9</sup>T. Ellenbogen, N. Voloch, A. Ganany-Padowicz, and A. Arie, *Nat. Photonics* **3**, 395 (2009).
- <sup>10</sup>A. Bruner, D. Eger, and S. Ruschin, *J. Appl. Phys.* **96**, 7445 (2004).
- <sup>11</sup>G. P. Agrawal, *Nonlinear Fiber Optics* (Academic, Boston, 1995).
- <sup>12</sup>I. Dolev, A. Ganany-Padowicz, O. Gayer, J. Mangin, G. Gadret, and A. Arie, *Appl. Phys. B: Lasers Opt.* **96**, 423 (2009).